Fixed-Wing UAV Guidance Law for Surface-Target Tracking and Overflight

Niki Regina
DEIS
University of Bologna
Via Fontanelle 40 Forli' 47100 Forli', Italy
+39-0543-786931
niki.regina2@unibo.it

Matteo Zanzi
ARCES
University of Bologna
Via Fontanelle 40 Forli' 47100 Forli', Italy
+39-0543-786933
matteo.zanzi@unibo.it

***Abstract*—This study presents a new guidance algorithm for a fixed-wing Unmanned Aerial Vehicle (UAV) used for surveillance tracking purposes. In particular, the algorithm ensures continual overflying of the target whether it is fixed or in motion. Attention was paid to the definition of the guidance specifications in order to derive a suitable guidance algorithm capable of fulfilling the requirements under tight constraints including the constancy of airspeed and bounded lateral accelerations. An assessment of the performance of the presented algorithm is given by means of hardware-in-the-loop tests.**

TABLE OF CONTENTS

1. INTRODUCTION

During the past decade, a growth in UAV technologies has made possible different tasks. One of the most important is the capability of the air vehicle to track a moving ground target through the use of a gimbaled camera. Usually a gimbals operator on the ground selects a target of interest using a joystick that moves the gimbaled camera. Once the target is selected the UAV and camera automatically track the target. This kind of system also performs a real time estimation of the target's velocity using UAV-gimbal telemetry data and the extracted target position on the image plane. Information about this scientific theme is available in Ref. [1], [2] and in Ref. [3] where similar approaches are presented.

In this paper the target is assumed to be friendly and its position known by the pursuer guidance system. The target position is assumed to be determined by the target itself and transmitted via data-link to the flying pursuer. It is an aim of the pursuer UAV to autonomously follow the target during its maneuvers, by avoiding to go too far away from it, as well as if the UAV is kept in a virtual leash by the target.

The aim of this paper is to develop a guidance law able to ensure a continuous loitering over the target when it is keeping still and to create a bounded trajectory around the position of the target when it moves.

In order to create a guidance algorithm two main different scenarios are described in literature:

1. The UAV flies autonomously along a predefined trajectory created on the fixed position of the target;
2. The UAV creates by itself a trajectory around the moving target.

For the first scenario a representative guidance law design technique recently presented in literature is the Lyapunov vector field (see Ref. [4], [5]). An inner feedback control loop is assumed to ensure the vehicle tracks the vector field by actuating the aircraft control surfaces in order to produce aerodynamics moments to achieve the desired vehicle attitude and altitude hold mode. The direction and the magnitude of the computed vector field velocity are transformed by the guidance outer loop into heading commands, suitable to assure the maneuvers of the UAV to be consistent to its flight performances in terms of minimum required air-speed and maximum turn-rate. In Ref. [6] a vector field for continuous live sensing is created through the use of a particular figure known as Lemniscate. Within the first scenario also the design techniques based on a imaginary point moving along the predefined trajectories must be included. This point is called pseudo-target or ghost-target. This approach is used in Ref. [7], [8] and [10] (here a 3D tracking is considered) where a guidance method for tracking straight line and curved path is presented. This guidance law is similar to a pure-pursuit guidance described in Ref. [9].

An hybrid solution is presented in Ref. [11], [12] and [13]. In these papers an oscillatory ghost-target is created around the moving or fixed position of the target. Consequently the UAV is forced to track the factious target by different guidance laws. This approach is definitely an improvement respect to the approaches cited until now although neither of them consider the problem of out-of-frame target images.

With reference to the second scenario, the guidance laws presented in Ref. [14] are able to track a moving target with a fixed horizontal range chosen by the operator. Besides, it is able to track the target even if it is out-of-frame. One of the limit of this guidance law is when the horizontal range is equal to zero due to disturbances, for instance.

The guidance law presented in Ref. [15] solves this problem. It can be seen in the simulations that, even if the distance is chosen equal to zero, the UAV stabilizes itself on a circle

[1] 978-1-4577-0557-1/12/$26.00 ©2012 IEEE.
[2] IEEEAC Paper #1126, Version 3, Updated 02/01/2012.

whose radius meets the UAV dynamics (see Ref. [16])

In this paper, using an approach similar to the last two cited articles, a new non-linear two dimension (2D) guidance law is presented. It generates petal-like trajectories along an horizontal plane at an established flight altitude, centered around a ground target, that ensures a continuous loitering over the target whether it keeps still or moves. The main features of the proposed law are twofold: its simplicity and adaptability to various tracking scenarios. In fact, according to this law, the UAV does not follow a path with a predefined shape created around the target; rather, it creates a trajectory whose points are computed in real time by the UAV itself depending on target available position and velocity data.

Similarly as in most flight applications, a separate inner and outer feedback-loop control approach is assumed in this work. This because of its simplicity and the availability of good autopilots for attitude stabilization and altitude hold. The outer guidance loop transforms the lateral acceleration computed by the guidance law into heading commands. The guidance law is suitable to guarantee the maneuvers of the UAV to be consistent to its flight performances in terms of minimum required air-speed and maximum turn-rate. The computation of the guidance law requires the knowledge of the UAV/Target Line-Of-Sight (LOS) and the LOS rate. Moreover, a few parameters have to be chosen and tuned according to the UAV flight performances and mission requirements (related to target over-flying repetition rate).

The significance of the proposed guidance algorithm respect to the existing ones consists in the fact that no fuel, time or distance-based cost function are minimized by the control law; instead, it allows a UAV for the continuous overflight of a target without the need of the design of a predefined trajectory.

Results are shown by providing simulations and tests. Numerical simulations of different tracking scenarios are proposed in order to show the behavior of the law, also taking into account wind effect. Besides, tests with a well known X-Plane 6DoF simulator are accomplished in order to evaluate the realistic behavior of the implemented guidance law on an existing aerial vehicle.

The paper is organized as follows. Section 2 describes the mathematical model of the target tracking problem. Section 3 presents the proposed guidance law and its main features. Section 4 is dedicated to the target velocity estimation. In section 5 some simulation results in order to evaluate the effectiveness of the law. Section 6 implements the proposed guidance law on X-Plane 6DoF simulator.

2. MODEL OF THE TARGET-TRACKING PROBLEM

In order to develop a guidance law for a fixed-wing UAV that tracks a ground target, some assumptions have been stated in this work. Firstly, the motion of the UAV is considered at constant altitude, herein the problem can be considered a two dimensional (2D) tracking problem. Moreover, the airspeed of the UAV is assumed to be constant in order to provide the necessary lift to hold the altitude as much as possible. Besides, the control input of the airplane is the lateral acceleration caused by aileron deflections and the lateral acceleration in its turn gives raise a heading change. Herein the UAV has been modeled as a mass-point moving on a horizontal plane according to the following mathematical model:

$$\begin{cases} \dot{x} = V\cos(\psi) + W_x \\ \dot{y} = V\sin(\psi) + W_y \\ \dot{\psi} = \frac{a_n}{V} \end{cases} \tag{1}$$

where $[x,\ y,\ \psi]^T$ is the state vector of the UAV model and the state variables represent the two Cartesian position coordinates along a North-East reference frame and the heading angle, respectively. W_x and W_y are the wind velocity components. The angle ψ is positive in an anti-clockwise sense and it represents the angle between the x (North) axis and the longitudinal UAV axis; this, in turn, coincides with the direction of the UAV airspeed vector $\mathbf{V}$ because no sideslip angle is considered. V is the norm of $\mathbf{V}$. a_n is the single input signal of the model and represents the value of lateral acceleration, i. e. the acceleration of the air vehicle perpendicular to its longitudinal axis. No longitudinal acceleration respect to the air flow is considered because $\dot{V} = 0$. As told before, the effect of the lateral acceleration is to cause a change in the rate of turn while leaving the airspeed unchanged.

In case of no wind the heading angle coincides with the course angle χ, i.e. the ground-track velocity-vector angle respect to the North direction.

In a target tracking problem is interesting to analyze the evolution of the geometry of relative target-pursuer motion rather than the position of the single points. In particular, according to [9] , the behavior of the projection of the relative target-pursuer distance on the horizontal plane, R, together with the Line-Of-Sight (LOS) angle σ, is described by the following dynamic model:

$$\begin{cases} \dot{R} = V_T\cos(\sigma - \chi_T) - V_G\cos(\sigma - \chi) \\ R\dot{\sigma} = -V_T\sin(\sigma - \chi_T) + V_G\sin(\sigma - \chi) \end{cases} \tag{2}$$

where V_T and χ_T are the target speed and course angle, respectively, while V_G is the UAV ground speed, R is the target-UAV distance.

Of course there is a relationship between model (1) and (2). In fact, $V_G = \sqrt{\dot{x}^2 + \dot{y}^2}$ and $R = \sqrt{(x - x_T)^2 + (y - y_T)^2}$, with $[x_T, y_T]^T$ the position coordinates of the target; moreover, $\tan\chi = \dot{y}/\dot{x}$.

A representation of the involved variables is given in figure 1.

As a consequence of the above discussion is $V_G = V_G(\psi, W_x, W_y)$ where

$$V_G(\psi, W_x, W_y) \equiv \sqrt{(V\cos(\psi) + W_x)^2 + (V\sin(\psi) + W_y)^2} \tag{3}$$

and, by defining the track angle

$$g(\psi, W_x, W_y) \equiv \arctan 2\,(V\sin(\psi) + W_y, V\cos(\psi) + W_x) \tag{4}$$

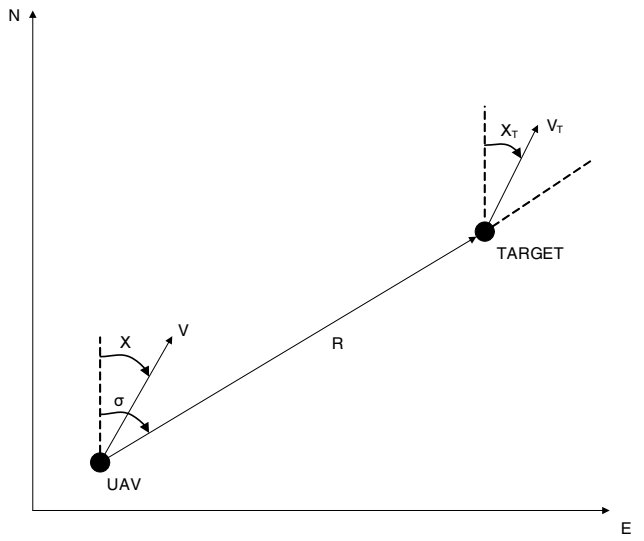

Figure 1. Target-Pursuer Relative Geometry

where $z = \arctan 2\,(b, a)$ is the usual four-quadrant arc tangent function such that $\tan\left(\arctan 2(b, a)\right) = \frac{b}{a}$, it is

$$\chi = g(\psi, W_x, W_y) \tag{5}$$

For the discussion in the next section it is also worth noting that

$$g\left(\psi, 0, 0\right) = \psi \tag{6}$$

and

$$V_G(\psi, 0, 0) = V \tag{7}$$

Finally, a mathematical model suitable for the UAV-Target tracking problem studied in this work is obtained by using eq. (1), eq. (2), eq. (3) and eq. (5) that yield to:

$$\begin{cases} \dot{R} = V_T \cos(\sigma - \chi_T) - \\ -V_G(\psi, W_x, W_y) \cos(\sigma - g(\psi, W_x, W_y)) \\ \\ R\dot{\sigma} = -V_T \sin(\sigma - \chi_T) + \\ +V_G(\psi, W_x, W_y) \sin(\sigma - g(\psi, W_x, W_y)) \\ \\ \dot{\psi} = \frac{a_n}{V} \end{cases} \tag{8}$$

Model (8) is a third order dynamic model where $[R, \ \ \sigma, \ \ \psi]^T$ is the state vector, a_n is the input, V_T and χ_T are time varying parameters, V, W_x and W_y are constant parameters.

3. PROPOSED GUIDANCE LAW

For the development of the guidance law the position and velocity of the target are assumed to be known by the UAV guidance system. (In [17] and [18] a description of typical sensors useful for this aim are given. Next section explains how position and velocity estimations are accomplished for the particular mission considered in this work). Then, the state of system (8) is observable. Moreover, the wind velocity is assumed to be known. According to this hypothesis, in eq. (8) V_T, χ_T, W_x and W_y can be considered as measurable parameters.

The requirements of the problem of guidance here considered can be summarized as follows.

The UAV has to track the target continuously. In order to do this, its airspeed is not lower than the target ground speed; rather, its airspeed is almost always greater then that of the target. As a consequence of this, the UAV usually reaches and overflies the target: hence a maneuver for turning back on the target after an overtaking is necessary.

The turning back has to be accomplished through turn rates compliant with the mechanical characteristics of the aircraft, and lateral accelerations required for these maneuvers have to be bounded. As previously recalled, during all the tracking maneuvers the airspeed of the UAV has to be maintained unchanged.

In order to derive a guidance law fulfilling the stated requirements, it can be designed according to the following specifications.

At first, the guidance law has to act on the lateral acceleration a_n, the only one controllable input of the system. The guidance law has to provide bounded signals.

Moreover, the guidance law has to steer the UAV towards the target when the UAV is approaching it. In this, the guidance law has to behave as a typical proportional navigation guidance. In particular, the guidance law has to be a function of the angle among the LOS and UAV ground velocity vector, i.e. $\sigma - \chi$.

Nevertheless, during overflying and after, the guidance law needs to give the UAV time sufficient to move away the target enough in order to gain the necessary range to be able to:

- turn back with a maneuver not so strong as to require an excessive lateral acceleration, that is to let admissible curvature radii;
- come back by heading toward the target avoiding to remain trapped on a loitering circle with a fixed radius around the target itself. This specification is necessary to avoid behaviors that imply steady limit cycles as in [15].

The proposed guidance law has therefore the following form:

$$a_n = K_1(R, \dot{R}) \arctan(K_2(\sigma - \chi)) \tag{9}$$

where

- $K_1() : \mathbb{R}^+ \times \mathbb{R} \to \mathbb{R}^+$;
- K_2 is a positive constant owning to the interval]0,1]

Function K_1 acts as a state-dependent gain that modulates the strength of the lateral acceleration provided by the guidance law. It acts according to the following criterion: when the UAV is going away after overflying the target but is yet near it within a circular area specified by a predefined radius R_0, the gain must be at its lowest value; otherwise it reaches its maximum value.

While it is possible to find out a smooth version of gain K_1, a discrete behavior has been selected in this work in order to evaluate the overall performances of the guidance law. Hence, the gain function is specified in table 1.

Table 1. Gain Selection for the Guidance Mode

	$R < R_0$	$R \geq R_0$
$\dot{R} < 0$	C	C
$\dot{R} \geq 0$	0	C

with $C \in \mathbb{R}^+$. Value of C and R_0 have to be selected by a tuning phase, even if an analytical approach is possible.

In fact, it must be highlighted that the proposed guidance law (9) is bounded and its maximum value is

$$|a_n|_{max} = C\frac{\pi}{2} \tag{10}$$

and it can be easily derived a formula for the gain C:

$$C = \frac{2}{\pi}|a_n|_{max} \tag{11}$$

It is also possible the equilibrium point of relative kinematic system and to derive a condition for K_2. In fact:

$$K_2 < \frac{2}{\pi}\tan(\frac{V^2}{CR_0}) \tag{12}$$

Remark

In order to have a reference value for the maximum lateral acceleration, it is worth noting that: by considering a plane flying along constant rate turn manouveour, it experiences a lateral acceleration given by $\frac{V^2}{R}$ *where* R *is the turn radious. Hence, the maximum value for the lateral acceleration can be chosen from this expression by selecting a suitable minimum value for* R_{min}*. That is:*

$$|a_n|_{max} = \frac{V^2}{R_{min}} \tag{13}$$

Moreover, by considering the well known flight mechanical equation for the coordinate turn [19] is

$$g\tan(\phi) = \frac{V^2}{R} \tag{14}$$

where ϕ *is the roll angle. By selecting a maximum roll angle value* $\phi_{max} = |\phi|_{max}$ *for a chosen UAV, it is possible to compute an expression for the minimun value for turn radious* R_{min}*.*

$$R_{min} = \frac{V^2}{g\tan(\phi_{max})} \tag{15}$$

As it has been discussed in the previous sections, the aim of this guidance law is to ensure with a fixed position of the target a continuos over-loiter on it. For this reason the equilibrium points which would drive the UAV on a circle trajectory must be avoided. To this aim $R < R_0$ must hold. Hence, from eq. (12) and the considerations presented in the remark it holds:

$$K_2 > \frac{2}{\pi}\tan(\frac{\pi R_{min}}{2R_0}) \tag{16}$$

As a consequence the new condition $R_{min} < R_0$ can be derived in order to satisfy eq. (16).

4. TARGET VELOCITY ESTIMATION

In order to compute the guidance law, the position and velocity vectors of both the UAV and the ground target are necessary. Position and velocity of the UAV are available from on-board sensors (like a GPS receiver); in this context the position of the target is assumed to be transmitted from ground, while the target velocity is assumed to be unknown. This is mainly due to limit the data-link bandwidth.

The availability of position and velocity information allows for the determination of the parameters used in the computation of the guidance law according to the following relationships:

$$\vec{R} = [x_T - x, y_T - y]^T, R = \left\|\vec{R}\right\|$$

$$\tan(\sigma) = \frac{x_T - x}{y_T - y}$$

$$\vec{V}_G = [\dot{x}, \dot{y}]^T, \vec{V}_T = [\dot{x}_T, \dot{y}_T]^T, \vec{V}_R = \vec{V}_T - \vec{V}_G$$

where $\vec{V}_R$ indicates the target-UAV relative velocity; moreover it can be easily verified that the following expression holds

$$\dot{R} = \frac{\vec{R}\cdot\vec{V}_R}{\|\vec{R}\|}$$

Hence, a filter capable to provide an estimate of the target velocity, together with a smoothed target position information, is needed on-board.

Many filters proposed for this task exist in literature based on variations of Kalman filters (EKF, Unscented, Particle filters, etc.): unfortunately the robustness of the estimation process remains usually a critical problem. Here a simple filter structure is given: its derivation is partially based on the idea of the fast estimator described in [14].

The filter has to estimate the North and East components of target position and velocity: due to the fact that North and East coordinates are de-coupled, only one channel of the filter is described here, the other one being similar.

The mathematical model of the process to be observed is:

$$\begin{cases} \dot{x}_T = u \\ y = x_T \end{cases} \tag{17}$$

where u denotes the target unknown North velocity, x_T is the target North position, y is the measurement received onboard. The proposed filter is illustrated in figure 2 where the hat over the variables indicate the corresponding estimated values. $R(s)$ is a transfer function to be selected in order to make the filter estimation process convergent.

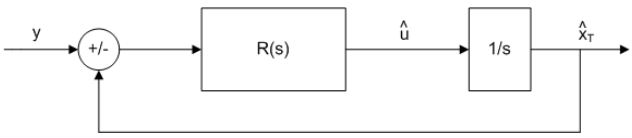

Figure 2. Target velocity estimation scheme

The updating equations of the filter, expressed in the s-domain, are:

$$\hat{x}_T(s) = \frac{R(s)\frac{1}{s}}{1 + R(s)\frac{1}{s}} y(s) \tag{18}$$

$$\hat{u}(s) = \frac{R(s)}{1 + R(s)\frac{1}{s}} y(s) \tag{19}$$

and the velocity estimation error can be expressed by

$$\hat{u}(s) - u(s) = G(s)u(s) \tag{20}$$

where

$$G(s) = \frac{R(s)}{s + R(s)} - 1 \tag{21}$$

By choosing a first order stable transfer function of the type

$$R(s) = \frac{k}{s + c} \tag{22}$$

with k and c positive constants, it results that the filter is stable and the velocity estimation error is bounded.

In particular, by selecting $k = \frac{c^2}{4}$, the filter is a second order system with two coinciding poles. An error estimation bound is given by (see the appendix for the derivation of the results and for the definition of $\mathcal{L}_1$ and $\mathcal{L}_\infty$ norms):

$$\|\hat{u}_t - u_t\|_{\mathcal{L}_\infty} \leq \|e_{u0t}\|_{\mathcal{L}_\infty} + \|G(s)\|_{\mathcal{L}_1} \|u_t\|_{\mathcal{L}_\infty} \tag{23}$$

with $e_{u0}(t)$ being the free response of the system $G(s)$ to the initial estimation errors.

Because of the limited speed of the target, it is

$$\|u_t\|_{\mathcal{L}_\infty} \leq u_{max}$$

hence, from (23), by substuting the results in appendix, it holds

$$\|\hat{u}_t - u_t\|_{\mathcal{L}_\infty} \leq M + 2u_{max} \tag{24}$$

with

$$M = \frac{2}{c} B e^{\frac{e_{u0}(0)}{B} - 1}$$

$$B = \|\dot{e}_{u0}(0) + \frac{c}{2} e_{u0}(0)\|$$

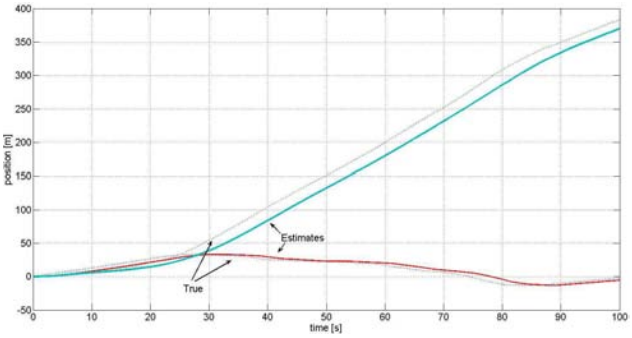

Figure 3. Distance with no wind effect

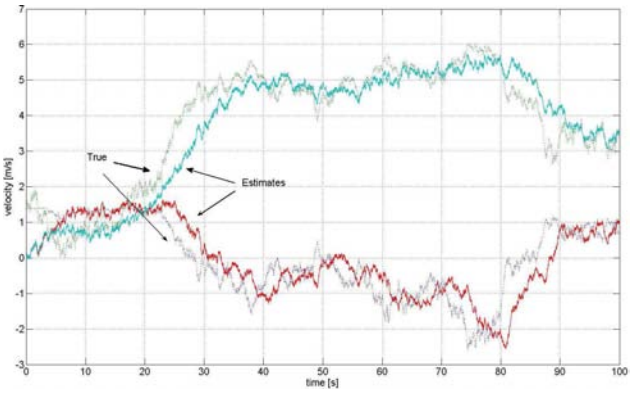

Figure 4. Distance UAV-Target with constant wind effect

5. Simulation Results

In this section several simulations results are presented in order to test the effectiveness of the guidance law presented in section 3. In these simulations the velocity of the UAV is considered constant at 10 m/s while, when the wind effect is considered, it has a constant east-direction and a constant speed equal to 3 m/s. The gains of the guidance law are: $C = 5$, $R_0 = 40$ and $K_2 = 1$. Three different cases are simulated, both with the target fixed and moving with different trajectories.

Through these simulations the effectiveness of the guidance law can be shown for all the possible motions of the target (fixed, moving with constant heading, moving with variable heading).

A. Fixed Target

In this first subsection the target is considered fixed in the origin and two different simulations are presented: the first one with no wind effect while the second with a constant wind. The initial position of the UAV is (100,100) with the initial heading pointing in north-east direction. The simulation lasts 100 s.

In figure 5 and 6 the continuous line represents the trajectories of the UAV while the star in the origin is the fixed target position. In figure 5 no wind effect are considered and the main

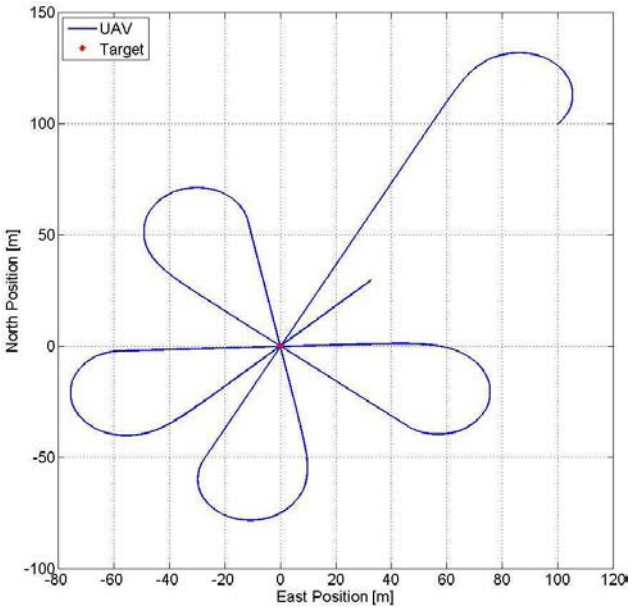

Figure 5. Trajectories of UAV with No Wind Effect

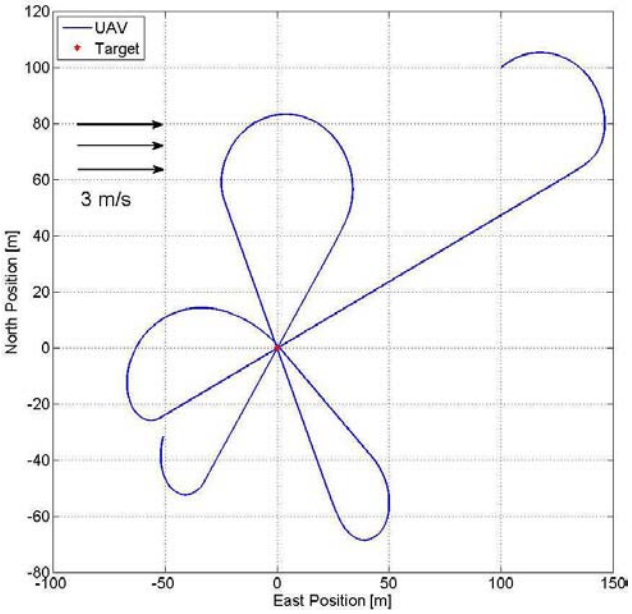

Figure 6. Trajectories of UAV with constant Wind Effect

charateristic of the guidance law designed are highlighted: the UAV is able to always pass over the target. In fig. 6 the trajectory of the UAV in presence of wind effect are shown. In this case the UAV is also able to pass over the target but with a different trajectory.

These considerations are also documented in fig. 7 and 8 where in both cases the distance between the UAV and the target goes periodically to zero. The only slight difference that can be seen between the two figures is the period of interception. Considering wind effects the period is longer. This could be an advantage when the trajectory will be implemented on the 6DoF flight simulator because the lateral acceleration required is smaller.

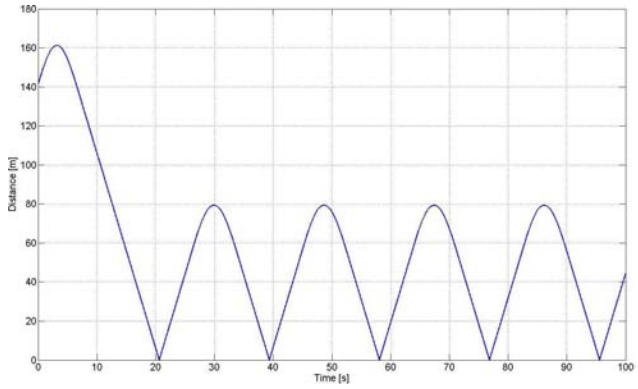

Figure 7. Distance UAV-Target with No Wind Effect

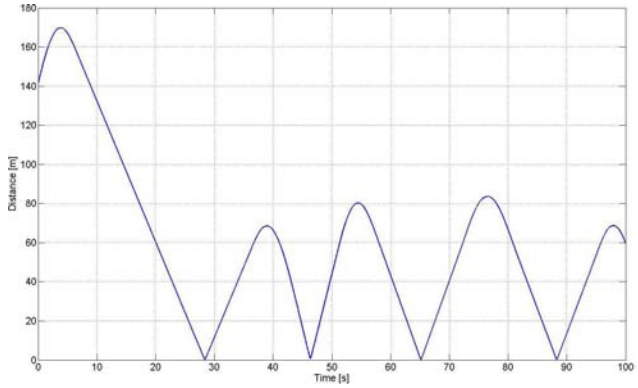

Figure 8. Distance UAV-Target with constant Wind Effect

B. Straight-line Target

In this case the target is supposed with a fixed north heading direction in order to create a straight-line trajectory. However, the speed of the target is variable always slower than the UAV cruise airspeed. The target's profile velocity is shown in fig. 9 where, again, from 70 to 250 s the target is considered fixed. It can be seen that the maximum velocity supposed is 7 m/s. As in the previous case, the simulations are presented with and without wind effect.

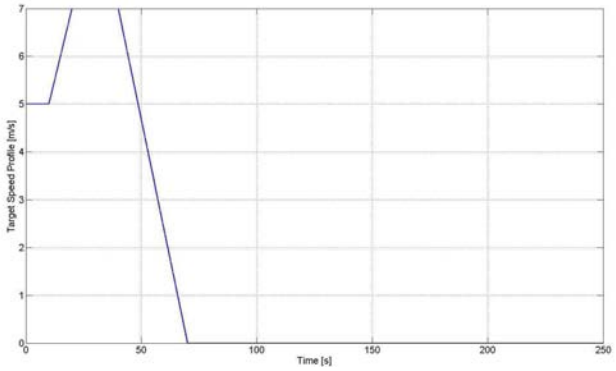

Figure 9. Target Velocity Profile

The trajectories of the UAV and the target are represented by, respectively, the blue line and the red line in fig. 10. In both cases, through the use of the guidance law designed, the UAV is able to track the target. Moreover, when the target is fixed the UAV flies over the pursuer continuously. The

different trajectories created by the guidance law are due to the presence of the wind.

Without the wind effect the trajectory in similar to a constant oscillation around the position of the target until it stops (see fig. 10). Observing fig. 11 it can be seen that the UAV, due to the presence and the direction of the wind that reduce the speed of the air-vehicle, points its heading behind the target. However, also in this case, the UAV starts to loiter around the final point reached by the target.

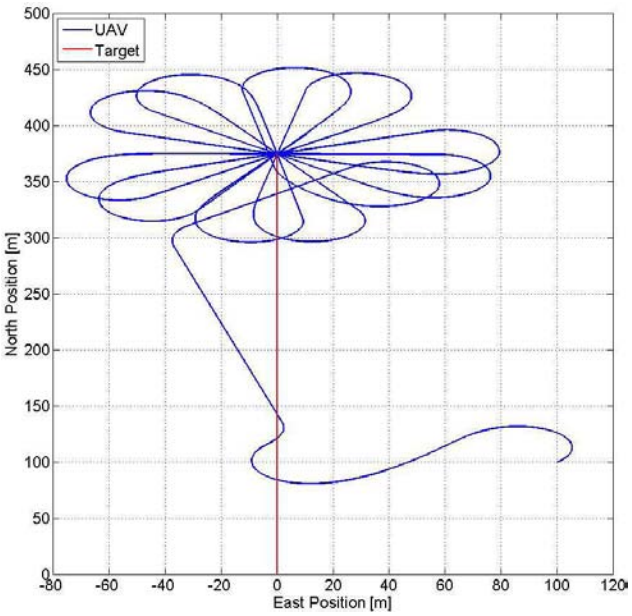

Figure 10. Trajectories of UAV with no wind effect

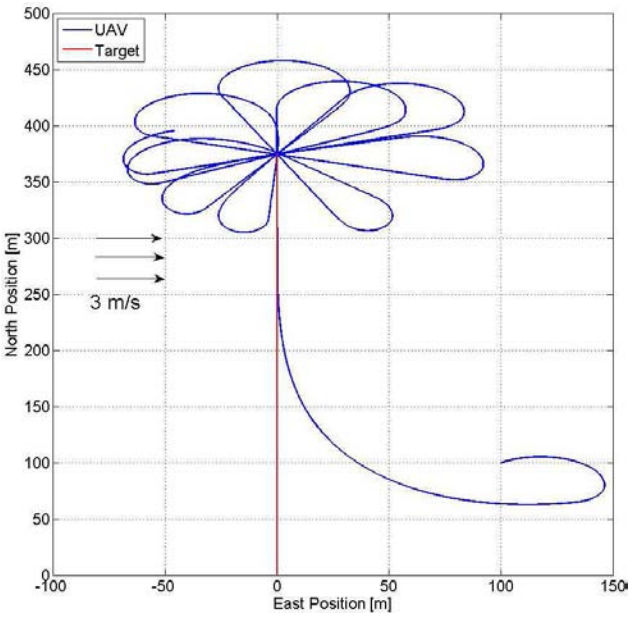

Figure 11. Trajectories of UAV with constant wind effect

Figure 12 shows the distance between the target and the UAV during the simulation. In fig. 12 the oscillation motion is shown in the first 50 s where the distance between the target and the UAV never goes to zero. Once the target stops itself the distance goes, again, periodically to zero. Figure 13 shows how the UAV intercept the target just before 50^{th} s, avoiding the oscillation motion. Once the UAV reaches the target it starts to loiter around the target as it is shown in the previous case.

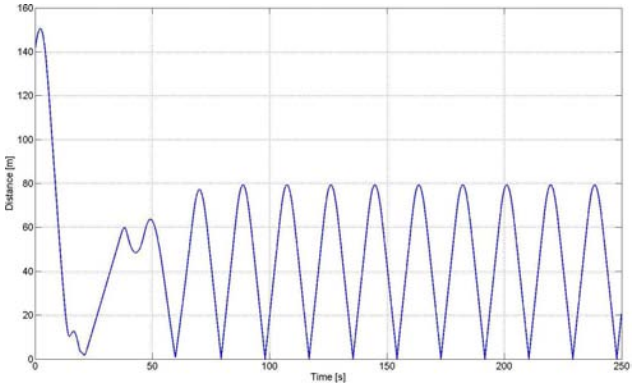

Figure 12. Distance with no wind effect

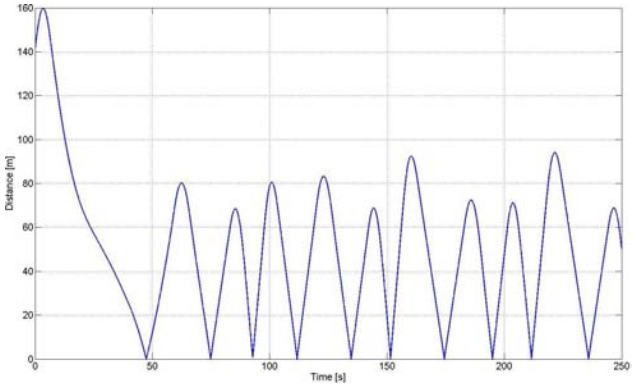

Figure 13. Distance UAV-Target with constant wind effect

C. Circular Target

In order to complete the simulations of the proposed guidance law, a circular trajectory is supposed for the target. The aim of this simulations is to test the guidance law when the target is completing a bend trajectory. In this case the velocity of the target is supposed to be constant at 5 m/s, with a constant lateral acceleration equal to 0.05 m/s^2 and, as in the previous cases wind and no-wind simulations are shown.

The initial position of the UAV is (100,0) with north-east initial heading angle. The target is initially placed in the origin (0,0). The simulation lasts 100 s. In fig. 14 the continuous line represents the UAV trajectory while the dashed line is the target trajectory. Both in fig. 14 (without wind) and in fig. 15 (constant wind) it is shown that the UAV is able to intercept the target and starts to loiter around.

Figure 16 shows that the distance between the UAV and the target goes to zero. The periodic behavior cited in the previous case is confirmed here where the maximum distance between the target and the UAV is around 60 m. The target is intercepted with a constant period 25 s.

Figure 17 shows that the UAV is able to reach the target but, due to the presence of the wind, the trajectory created by the guidance law is not periodic anymore.

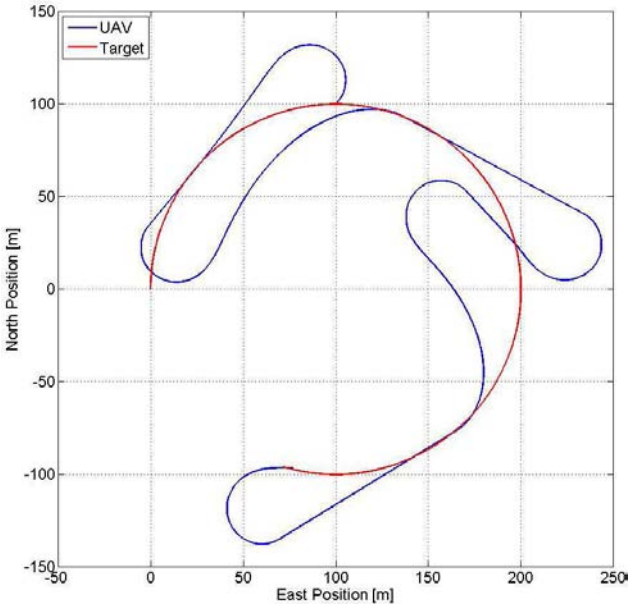

Figure 14. Trajectories of UAV with no wind effect

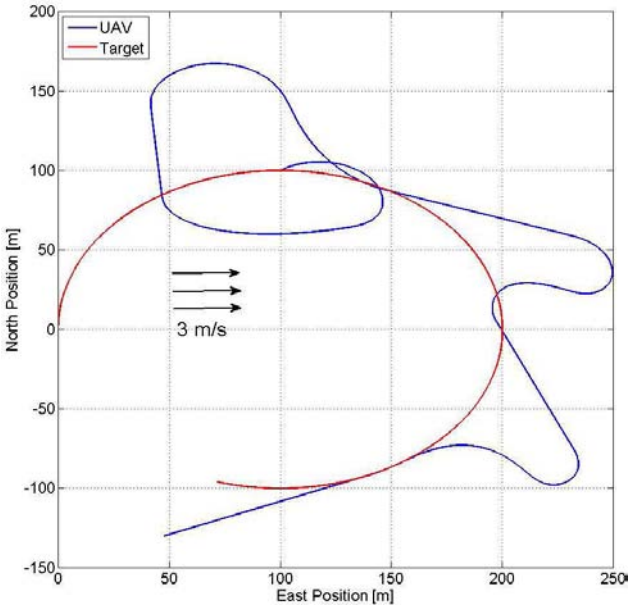

Figure 15. Trajectories of UAV with constant wind effect

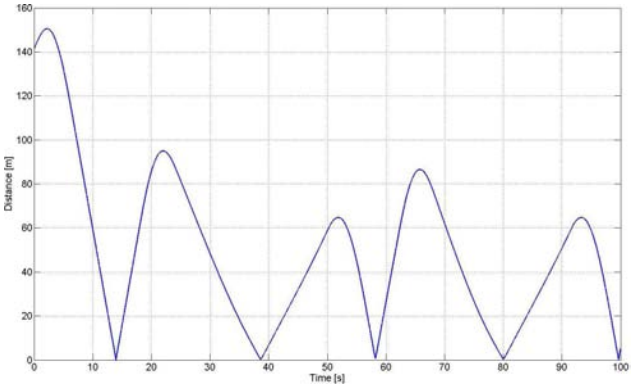

Figure 16. Distance with no wind effect

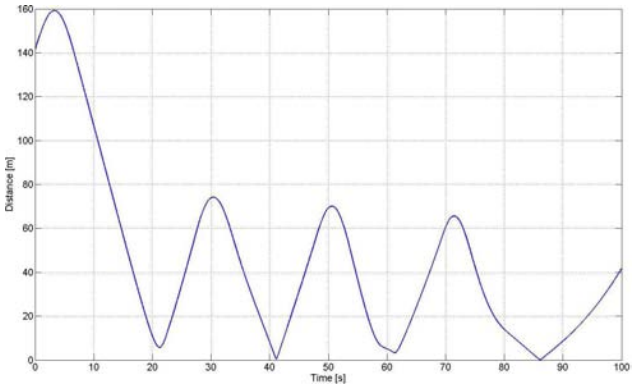

Figure 17. Distance UAV-Target with constant wind effect

Comments

In all the cases analyzed in this section (A, B, C) the guidance law designed has the expected behavior. In particular, the aim to create a guidance law able to fly over the target continuously is reached. Moreover, the fig. 10 and the fig. 16 shows that the guidance law ensures that the distance goes to zero also when the target is moving.

6. HIL ARDUPILOT SIMULATION

The proposed guidance law described in sec. 3, has been implemented on the board ardupilot-mega. One of the main features of this microcontroller is the open source firmware which can be easily modified by any user. In particular, the APM 2.12 source code has been changed to ensure a target tracking hardware in the loop (HIL) simulation. The setup is explained in fig.

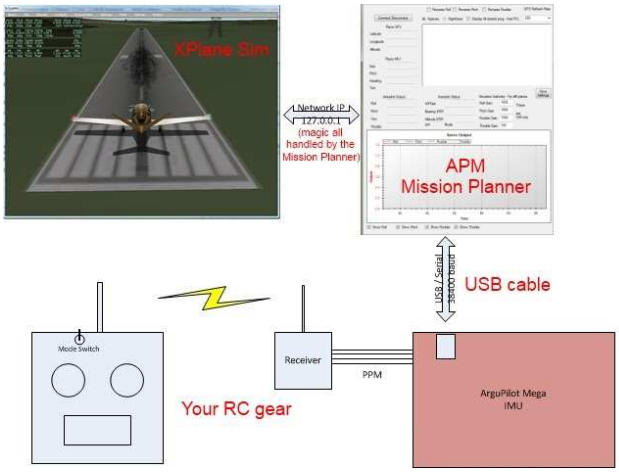

Figure 18. Setup of HIL simulation

The 6DoF flight simulator chosen for HIL simulation is X-Plane and, in order to have a more realistic simulation, the PT-60 RC airplane has been chosen as RC model aircraft. The charateristics of the plane are described in tab. 2.

Together with the APM source code, ardupilot-mega offers the chance to use the Mission Planner (known also as ground station) which serves as a bridge between the board and X-Plane. The ground station reads the data coming from the fligth simulator and sends it, through the serial port, to the APM. At the same time it sends the servo outputs calculated

Figure 19. GP-PT 60 RC model

UAV Model	GP-PT 60
Wing	
Span	5.4 $[ft]$
Mean Aerodynamic Chord	0.95 $[ft]$
Airfoil	NACA 2412
Incidence	0.0 $[deg]$
Aileron Deflection	$\pm 20[deg]$
Horizontal Stabilizer	
Span	1.85 $[ft]$
Mean Aerodynamic Chord	0.52 $[ft]$
Airfoil	NACA 0006
Incidence	8.5 $[deg]$
Elevator Deflection	$\pm 20[deg]$
Vertical Stabilizers	
Span	1.4 $[ft]$
Mean Aerodynamic Chord	0.5 $[ft]$
Airfoil	NACA 0009
Rudder Deflection	$\pm 20[deg]$

Table 2. GP-PT Geometric Characteristics

by the autopilot to X-Plane.

Two different simulations results are presented. In the first one a moving target has been simulated while in the second simulation a fixed target position has been chosen in order to highlight the main charateristic of the proposed guidance law to ensure a continuos over-loitering on it. Both the simulations are made with these parameters:

- Aircraft Cruise Speed V = 15 [m/s];
- Wind Speed 3 [m/s];
- Wind Direction 30;
- Desired radious 100 [m]
- C = 15, K_2 = 0.3.

Moving Target

In order to simulate a target tracking, a trajectory has been completed by a car and its data (position, speed and heading) sampled by a GPS receiver at 0.3 Hz. All these data has been implemented on ardupilot-mega and with different changes made to the APM 2.12 it has been possible to simulate the UAV that follows a moving target.

Figure 20 shows the 3D trajectory of the UAV. The yellow poiters represent the data sampled by the GPS's car while the red line is the trajectory completed by the UAV. It is also important to show the attitude (fig.21), the altitude and the distance between the UAV and the moving target (fig. 22).

As can be seen the UAV follows the target and its attitude shows a bounded roll angle and a stable pitch which can be also seen by the altitude profile. The distance plot shows sometimes values over 500 [m] but this is due to the speed reached by the ground target. It is obvious that if the target goes faster than the UAV the distance increases but it drops quickly around 150 [m] when the car decreases its speed.

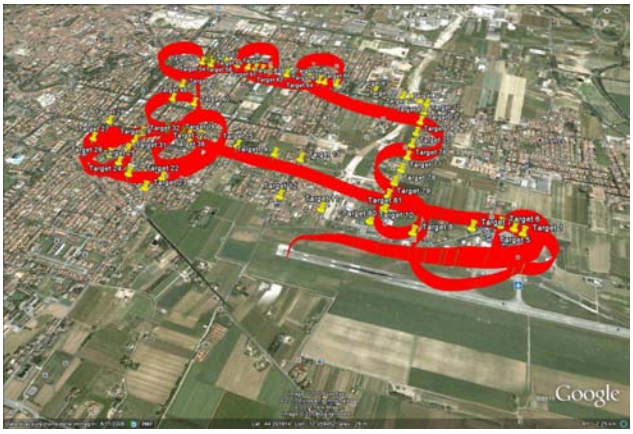

Figure 20. 3D HIL trajectories

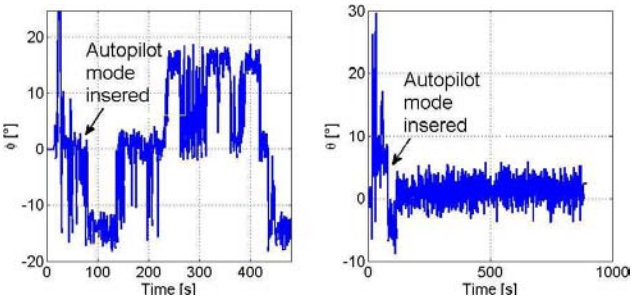

Figure 21. Roll and Pitch angles

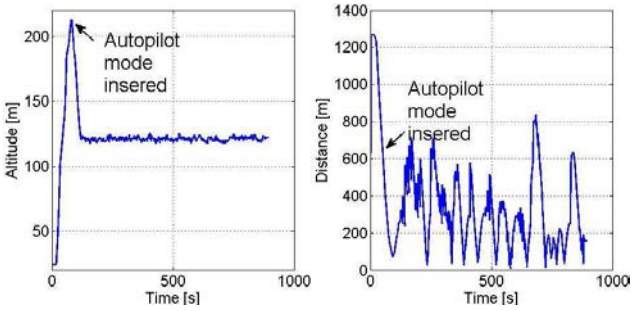

Figure 22. Height and Distance

Fixed Target

In this simulation a fixed target has been supposedly placed near Forl Airport. As can be seen a continuous over-loitering of the fixed point is performed by the UAV. As in the previous subsection the roll angle remains bounded as the pitch angle and the altitude. It is important to see how the distance goes close to zero cyclically.

Figure 23. 3D HIL trajectories

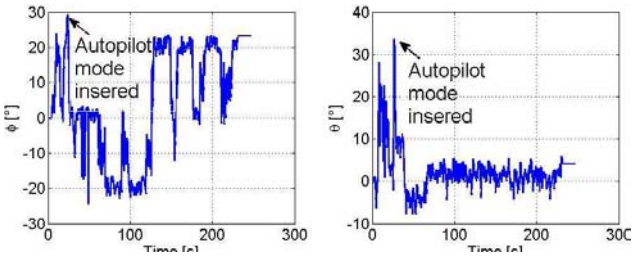

Figure 24. Roll and Pitch angles

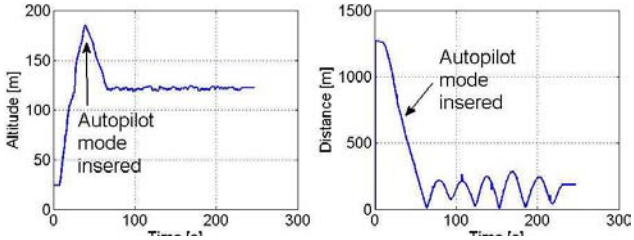

Figure 25. Height and Distance

APPENDICES

The definition of $\mathcal{L}_1$ and $\mathcal{L}_\infty$ norms is:

$$\|u_t\|_{\mathcal{L}_\infty} = \sup_{0\le\tau\le t} |u(\tau)|$$

$$\|G(s)\|_{\mathcal{L}_1} = \int_0^\infty |g(\tau)|\, d\tau$$

If the Input-Output model of a system in the s-domain is

$$y(s) = G(s)u(s) = \frac{-s(s+c)}{s(s+c)+k} \tag{25}$$

then the time response $y(t)$ is

$$y(t) = y_0(t) + \int_0^t g(\tau)u(t-\tau)d\tau \tag{26}$$

where $y_0(t)$ is the free response to initial conditions and $g(t)$ is impulse response od the system, obtained as the anti-transform of $G(s)$.

Hence, it holds

$$\|y_t\|_{\mathcal{L}_\infty} \le \|y_{0t}\|_{\mathcal{L}_\infty} + \left\| \int_0^t g(\tau)u(t-\tau)d\tau \right\|_{\mathcal{L}_\infty} \tag{27}$$

and, from (27),

$$\|y_t\|_{\mathcal{L}_\infty} \le \|y_{0t}\|_{\mathcal{L}_\infty} + \|G(s)\|_{\mathcal{L}_1} \|u_t\|_{\mathcal{L}_\infty} \tag{28}$$

If

$$G(s) = \frac{-s(s+c)}{s(s+c)+k} \tag{29}$$

by selecting $k = \frac{c^2}{4}$, $c > 0$, yields to

$$G(s) = -s\frac{(s+c)}{(s+\frac{c}{2})^2} \tag{30}$$

whose impulse response $g(t)$ is

$$g(t) = \delta(t) - \frac{c^2}{4} t e^{-\frac{c}{2}t} \tag{31}$$

where $\delta(t)$ is the Dirac impulse.

From easy passages the following expression can be obtained

$$\|G(s)\|_{\mathcal{L}_1} = \int_0^\infty |g(\tau)|\, d\tau = 2$$

Moreover, in this case the free response can be computed after some algebra and gives:

$$y_0(t) = (y_0(0) + Bt)e^{-\frac{c}{2}t} \tag{32}$$

with

$$B = \dot{y}_0(0) + \frac{c}{2} y_0(0)$$

$|y_0(t)|$ admits a maximum for $t > 0$ whose value is $M = \frac{2}{c}|B|e^{\frac{y_0(0)}{B}-1}$. Hence

$$\|y_{0t}\|_{\mathcal{L}_\infty} = M \tag{33}$$

REFERENCES

[1] I. Wang, V. Dobrokhodov, I. Kaminer, and K. Jones, "On vision-based tracking and motion estimation for moving targets using small uavs," in *Proceedings of Guidance Navigation and Control Conference*. San Francisco, CA, USA: AIAA, 2005.

[2] V. Dobrokhodov, I. Kaminer, K. Jones, and R. Ghabcheloo, "Vision-based tracking and motion estimation for moving targets using small uavs," in *Proceedings of Guidance Navigation and Control Conference*. Key Stone, CO, USA: AIAA, 2006.

[3] V. Dobrokhodov, I. Kaminer, K. Jones, I. Kistios., C. Cao, L. Ma, N. Hovakimyan, and C. Wosley, "Rapid motion estimation of a target moving with time-varying velocity," in *Proceedings of Guidance Navigation and Control Conference*. Hilton Head, SC, USA: AIAA, 2007.

[4] D. Nelson, B. Barber, T. McLain, and W. Bear, "Vector field path following for miniature airvehicle," *IEEE Transaction on Robotics*, vol. 23, no. 3, 2007.

[5] D. Lawreance, E. Frew, and W. Pisano, "Lyapunov vector field for autonomous uav flight control," in *Proceedings of Guidance and Navigation Control Conference*. Hilton Head, SC, USA: AIAA, 2007, pp. 6317 – 6339.

[6] N. Regina and M. Zanzi, "Uav guidance law for target tracking along a constrained bow-shaped trajectory based on lyapunov vector field," in *Proceedings of Symposioum on Aerospace Control Automation*. Nara, Japan: IFAC, 2010.

[7] S. Park, J. Deyst, and J. How, "A new nonlinear guidance logic for trajectory tracking," in *Proceedings of Guidance and Navigation and Control Conference*. Providence, Rhode Island: AIAA, 2004.

[8] ——, "Performance and lyapunov stability of a nonlinear path-following guidance method," *Journal of Guidance,Control and Dynamics*, vol. 30, no. 6, 2007.

[9] C. Lin, *Modern Navigation Guidance and Control Processing Vol.2*. Prentice Hall,Upper Saddle River (NJ), 1991.

[10] D. Gates, "Nonlinear path following method," *Journal of Guidance, Control and Dynamics*, vol. 33, no. 2, 2010.

[11] M. Zennaro and R. Sengupta, "Strategies of path-planning for a uav to track a ground vehicle," in *Proceedings of the AINS Conference*. Bologna, IT: AINS, 2003.

[12] E. Lalish, K. Morgansen, and T. Tsukamaki, "Oscillatory control for constant-speed unicycle-type vehicles," in *Proceedings of 46th IEEE Conference on Decision and Control*. New Orleans, LA, USA: IEEE, 2007, pp. 5246 – 5251.

[13] N. Regina and M. Zanzi, "Uav guidance law for ground-based target trajectory tracking and loitering," in *Proceedings of Aerospace Conference*. Big Sky, MT, USA: AIAA/IEEE, 2011.

[14] L. Ma, C. Cao, N. Hovakimyan, V. Dobrokhodov, and I. Kaminer, "Adaptive vision-based guidance law with guaranteed performace bounds," *Journal of Guidance, Control and Dynamics*, vol. 33, no. 3, 2010.

[15] N. Regina and M. Zanzi, "2d tracking and overflight of a target by means of nonlinear guidance law for uav," in *Proceedings of Aerospace Conference*. Big Sky, MT, USA: AIAA/IEEE, 2009.

[16] V. Dobrokhodov, I. Kaminer, K. Jones, and R. Ghabcheloo, "Vision-based tracking and motion estimation for moving targets using unmanned air vehicles," *Journal of Guidance, Control and Dynamics*, vol. 31, no. 4, 2008.

[17] K. ZuWhan and R.Sengupta, "Target detection and position likelihood using an aerial image sensor," in *Proceedings of International Conference on Robotics and Automation*. Pasadena, CA, USA: ICRA/IEEE, 2008.

[18] L. Bertuccelli and J. How, "Search for dynamic targets with uncertain probability maps," in *Proceedings of American Control Conference*. Minneapolis, MI, USA: IEEE, 2006.

[19] D. Raymer, *Aircraft Design: a conceptual approach*. AIAA Education Series, 1999.

BIOGRAPHY

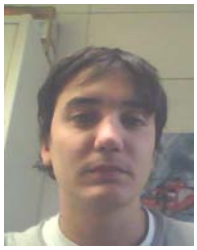

Niki Regina is a Ph.D researcher with the Department of Electronics, Computer Systems and Telecommunications (DEIS) of the university of Bologna. He was graduated in 2007 in Aerospace Engineering at the University of Bologna. His fields of interest concern guidance and control system on aerospace and nonlinear control.

Matteo Zanzi is a researcher with the ARCES research center of the University of Bologna. He was graduated in 1995 in Electrical Engineering and received the Ph.D degree in System Engineering in 1999 from the University of Bologna. His field of interest concerns navigation, guidance and control systems on aerospace. In particular, his area of expertise is satellite-based navigation for general aviation: data fusion between GPS and inertial sensors, guidance laws and integrity algorithms. He is assistant professor of Air Navigation Data Processing and Automatic Control Systems.